A Case Study in Collocation: Heat Transfer Effects in Cavitation Bubble Dynamics

Matthew Warnez
Faculty advisor: Eric Johnsen

2012 December 19

Contents

1 Introduction

Rapid fluctuations of pressure and temperature are common inside a cavitating bubble, but modeling the full temperature distribution inside the bubble creates a host of numerical challenges. In this study we will use a collocation method to solve the equations of cavitation bubble dynamics with only very few assumptions. These assumptions, namely uniform pressure inside the bubble and a spherical symmetry, allow use of the well-known Rayleigh-Plesset equation, but aim to have minimally deleterious effects on accuracy.

Collocation is a numerical method that can be used to solve partial differential equations. By expanding an unknown function into a linear combination of basis functions and evaluating this

function at a number of points in the domain, the weights of the basis functions can be solved for at each time step. The temperature distribution inside the bubble wall makes a good candidate for collocation.

2 Physical problem

2.1 Governing equations

The radial dynamics of the bubble are governed by Keller's equation, a variant of the Rayleigh-Plesset equation which accounts for effects of compressibility.

$$\left(1-\frac{\dot{R}}{c_L}\right)R\ddot{R}+\frac{3}{2}\left(1-\frac{\dot{R}}{3c_L}\right)\dot{R}^2=\frac{1}{\rho_L}\left(1+\frac{\dot{R}}{c_L}+\frac{R}{c_L}\frac{d}{dt}\right)[p_B-p_A] \tag{1}$$

R is the bubble radius, c_L is the sound speed in the surrounding liquid, ρ_L is the liquid density, p_B is the liquid pressure at the bubble wall, p_A is the far-field (ambient) pressure. Here, overdots denote derivatives with respect to time. The pressure inside the bubble, p, taken to be uniform throughout, is described by

$$\dot{p}=\frac{3}{R}\left((\gamma-1)\,\lambda\left.\frac{\partial T}{\partial r}\right|_R-\gamma p\dot{R}\right) \tag{2}$$

where $\lambda(T)$ is the thermal conductivity, T is the temperature, r is the distance from the bubble's center, and γ is the ratio of specific heats. The external pressure p_B is related to the internal pressure by a stress balance at the bubble's center, which gives

$$p=p_B+\frac{2S}{R}+\frac{4\mu_L\dot{R}}{R} \tag{3}$$

where S is the surface tension, and μ_L is the liquid viscosity. The temperature and the thermal conductivity inside the bubble is allowed to vary over space, and is governed by the equation

$$\frac{\gamma}{\gamma-1}\frac{p}{T}\left[\frac{\partial T}{\partial t}+\frac{1}{\gamma p}\left((1-\gamma)\lambda\frac{\partial T}{\partial r}-\frac{r\dot{p}}{3}\right)\frac{\partial T}{\partial r}\right]-\dot{p}=\nabla\cdot(\lambda\nabla T) \tag{4}$$

We make the "cold" liquid assumption

$$T(R,t)=T_\infty \tag{5}$$

that is, the bubble temperature at the bubble wall is fixed at the ambient liquid temperature, T_∞. It has been repeatedly shown that this is a reasonable approximation for liquids in the vicinity of room temperature.

2.2 Change of variables

We introduce the auxiliary variable

$$\tau=\int_{T_\infty}^{T}\lambda(T')dT' \tag{6}$$

so that

$$\nabla \cdot (\lambda \nabla T) = \nabla \cdot \left(\lambda \frac{\partial T}{\partial \tau} \frac{\partial \tau}{\partial r} \right) = \nabla \cdot \left(\lambda \frac{1}{\lambda} \frac{\partial \tau}{\partial r} \right) = \nabla^2 \tau \tag{7}$$

To approximate the dependence of thermal conductivity on temperature we use the linear relation

$$\lambda(T) = AT + B \tag{8}$$

where $A = 5.528 \cdot 10^{-5}\,\mathrm{J/m\,s\,K^2}$ and $B = 1.165 \cdot 10^{-2}\,\mathrm{J/m\,s\,K}$. This allows inversion of the definition of τ to find

$$T = \sqrt{\lambda_\infty^2 + 2A\tau} - \frac{B}{A} \tag{9}$$

where $\lambda_\infty = AT_\infty + B$.

Furthermore, we use the coordinate

$$x = \frac{r}{R} \tag{10}$$

to fix the domain for spatial discretization. In all that follows, $x = 0$ hence refers to the bubble center, while $x = 1$ refers to the bubble wall.

3 Collocation method

To solve for the temperature-like distribution τ over space and time, we use a collocation method. In this method, τ is expanded into a partial sum of time-dependent coefficients $a_n(t)$ multiplied into basis functions $\phi_n(y)$:

$$\tau(t, y) = \sum_{n=0}^{N} a_n(t) \phi_n(x) \tag{11}$$

The goal is to, at every time step, solve for the time-dependent coefficients such that τ accurately approximates the temperature-like distribution inside the bubble. We can write that

$$\frac{\partial \tau}{\partial t} = \sum_{n=0}^{N} \dot{a}_n(t) \phi_n(x) = f\left(x, R, p, \dot{p}, \frac{\partial \tau}{\partial x}, \frac{\partial^2 \tau}{\partial x^2} \right) \tag{12}$$

where the nonlinear function f results from equation (4) after the appropriate change in variables. By evaluating (12) at $N+1$ collocation points, a system of $N+1$ equations for the unknown collocation coefficients $a_0, \ldots, a_N$ is created.

If the basis functions $\phi_n(x)$ are chosen properly, then helpful expressions for the spatial-derivatives of τ can be extracted.

3.1 Chebyshev polynomial expansions

In this study, we will use the even Chebyshev polynomials of the first kind, $T_{2n}(x)$, as the basis functions. In what follows, we will derive all of the relations necessary to make effective use of the Chebyshev polynomials for collocation.

The Chebyshev polynomials are well known to abide by the derivative recurrence relation

$$2T_n = \frac{1}{n+1}\frac{dT_{n+1}}{dx} - \frac{1}{n-1}\frac{dT_{n-1}}{dx} \tag{13}$$

which can be alternatively written and expanded as

$$\begin{aligned}
\frac{d}{dx}T_{n+1} &= 2(n+1)T_n + \frac{n+1}{n-1}\frac{d}{dx}T_{n-1} && (14)\\
\frac{d}{dx}T_{2n} &= 2(2n)T_{2n-1} + \frac{2n}{2n-2}\frac{d}{dx}T_{2n-2} && (15)\\
&= 2(2n)T_{2n-1} + \frac{2n}{2n-2}\left(2(2n-2)T_{2n-3} + \frac{2n-2}{2n-4}\frac{d}{dx}T_{2n-4}\right) && (16)\\
&= 2(2n)T_{2n-1} + 2(2n)T_{2n-3} + \frac{2n}{2n-4}\frac{d}{dx}T_{2n-4} && (17)\\
&= 2(2n)T_{2n-1} + 2(2n)T_{2n-3} + \cdots + 2(2n)T_1 + (2n)\frac{d}{dx}T_0 && (18)\\
&= 4n\sum_{k=1}^{n} T_{2k-1} && (19)
\end{aligned}$$

since $dT_0/dx = 0$. This can be used to express the first spatial derivative of τ as a linear combination of the a_n coefficients.

$$\begin{aligned}
\frac{d\tau}{dx} &= \sum_{n=0}^{N} a_n \frac{dT_{2n}}{dx} && (20)\\
&= \sum_{n=0}^{N} a_n \left(4n\sum_{k=1}^{n} T_{2k-1}\right) && (21)\\
&= \sum_{n=1}^{N} e_n T_{2n-1} && (22)
\end{aligned}$$

where

$$e_n = 4\sum_{k=n}^{N} k a_k \tag{23}$$

Now from the original recurrence relation we consider that

$$\frac{dT_{2n-1}}{dx} = 2(2n-1)T_{2n-2} + \frac{2n-1}{2n-3}\frac{dT_{2n-3}}{dx} \tag{24}$$

$$= 2(2n-1)T_{2n-2} + \frac{2n-1}{2n-3}\left(2(2n-3)T_{2n-4} + \frac{2n-3}{2n-5}\frac{dT_{2n-5}}{dx}\right) \tag{25}$$

$$= 2(2n-1)T_{2n-2} + 2(2n-1)T_{2n-4} + \cdots + 2(2n-1)T_2 + (2n-1)\frac{dT_1}{dx} \tag{26}$$

$$= 2(2n-1)T_{2n-2} + 2(2n-1)T_{2n-4} + \cdots + 2(2n-1)T_2 + (2n-1)T_0 \tag{27}$$

$$= (2n-1)\sum_{k=1}^{n} f_k T_{2(k-1)} \tag{28}$$

where

$$f_k = \begin{cases} 1 & \text{if } k = 1 \\ 2 & \text{if } k \neq 1 \end{cases} \tag{29}$$

This allows us to write the second derivate of an even Chebyshev polynomial as

$$\frac{d^2T_{2n}}{dx^2} = 4n\sum_{k=1}^{n}\frac{dT_{2k-1}}{dx} \tag{30}$$

$$= 4n\sum_{k=1}^{n}\left((2k-1)\sum_{m=1}^{k} f_m T_{2(m-1)}\right) \tag{31}$$

$$= 4n\sum_{k=1}^{n} c_{k,n} T_{2(k-1)} \tag{32}$$

where

$$c_{k,n} = f_k \sum_{m=k}^{n}(2m-1) \tag{33}$$

The second derivate of $\tau(t, y)$ can be written

$$\frac{\partial^2\tau}{\partial x^2} = \sum_{n=1}^{N} e_n \frac{dT_{2n-1}}{dx} \tag{34}$$

$$= \sum_{n=1}^{N} d_n T_{2n-2} \tag{35}$$

where

$$d_n = f_n \sum_{k=n}^{N}(2k-1)e_k \tag{36}$$

In a similar way it can be shown that

$$\frac{d^3T_{2n}}{dx^3} = 16n\sum_{k=2}^{n}\left(\sum_{m=k}^{n} c_{m,n}(m-1)\right)T_{2n-3} \qquad n = 2, 3, \ldots \tag{37}$$

and that

$$\frac{\partial^3 T_{2n}}{\partial x^3} = \sum_{n=1}^{N} d_n \frac{dT_{2n-2}}{dx} \tag{38}$$

$$= \sum_{n=1}^{N} d_n \left(4(n-1) \sum_{k=1}^{n-1} T_{2k-1} \right) \tag{39}$$

$$= \sum_{n=2}^{N} 4d_n(n-1) \sum_{k=2}^{n} T_{2k-3} \tag{40}$$

$$= \sum_{n=2}^{N} g_n T_{2n-3} \tag{41}$$

where

$$g_n = \sum_{k=n}^{N} 4d_k(k-1) \tag{42}$$

$$\tag{43}$$

3.2 Implementation

At some time t, let $\boldsymbol{\tau}(t)$ be a vector in which each component is the temperature-like variable τ evaluated at a unique collocation point. To avoid Runge's phenomenon, we use the collocation points given by the Gauss-Lobatto quadrature points

$$x_k = \cos \frac{\pi k}{2N}, \quad k = 0, 1, \ldots, N \tag{44}$$

giving

$$\boldsymbol{\tau} = \begin{bmatrix} \tau(t, x_0) \\ \tau(t, x_1) \\ \vdots \\ \tau(t, x_N) \end{bmatrix} \tag{45}$$

Now if we let A be the collocation matrix defined by

$$A = \begin{bmatrix} T_0(x_0) & T_2(x_0) & \cdots & T_{2N}(x_0) \\ T_0(x_1) & T_2(x_1) & \cdots & T_{2N}(x_1) \\ \vdots & \vdots & \ddots & \vdots \\ T_0(x_N) & T_2(x_N) & \cdots & T_{2N}(x_N) \end{bmatrix} \tag{46}$$

and $\mathbf{a}(t)$ be the coefficient vector

$$\mathbf{a} = \begin{bmatrix} a_0(t) \\ a_1(t) \\ \vdots \\ a_N(t) \end{bmatrix} \tag{47}$$

then

$$\boldsymbol{\tau} = A\mathbf{a} \tag{48}$$

Note that the entries in A can easily be computed from the Chebyshev polynomial property that

$$T_{2n}(y_m) = \cos\left(2n \arccos y_m\right) \tag{49}$$

To compute the first spatial derivative of $\boldsymbol{\tau}$ we define

$$B = \begin{bmatrix} T_1(y_0) & T_3(x_0) & \cdots & T_{2N-1}(x_0) \\ T_1(x_1) & T_3(x_1) & \cdots & T_{2N-1}(x_1) \\ \vdots & \vdots & \ddots & \vdots \\ T_1(x_N) & T_3(x_N) & \cdots & T_{2N-1}(x_N) \end{bmatrix} \tag{50}$$

and note that from equation (23)

$$e_n = 4 \begin{bmatrix} 0 & \cdots & 0 & n & n+1 & \cdots & N \end{bmatrix} \begin{bmatrix} a_0 \\ a_1 \\ \vdots \\ a_{n-1} \\ a_n \\ a_{n+1} \\ \vdots \\ a_N \end{bmatrix} \tag{51}$$

Therefore

$$\mathbf{e} = \begin{bmatrix} e_1 \\ e_2 \\ e_3 \\ \vdots \\ e_N \end{bmatrix} = 4 \begin{bmatrix} 0 & 1 & 2 & 3 & \cdots & N \\ 0 & 0 & 2 & 3 & \cdots & N \\ 0 & 0 & 0 & 3 & \cdots & N \\ \vdots & \vdots & \vdots & \vdots & \ddots & \vdots \\ 0 & 0 & 0 & 0 & \cdots & N \end{bmatrix} \begin{bmatrix} a_0 \\ a_1 \\ a_2 \\ a_3 \\ \vdots \\ a_N \end{bmatrix} \tag{52}$$

Defining the matrix in (51) to be $E/4$, the value of $\partial\tau/\partial y$ at each collocation point is given by

$$\frac{\partial \boldsymbol{\tau}}{\partial y} = BE\boldsymbol{a} \tag{53}$$

By a similar process, a matrix D generated from the values of d_n given in equation (36) allows the second derivative to be written

$$\frac{\partial^2 \boldsymbol{\tau}}{\partial y^2} = AD\boldsymbol{a} \tag{54}$$

In fact, any spatial derivative of $\boldsymbol{\tau}$ can be written as a linear transformation on the coefficients vector $\boldsymbol{a}$. In the appendix we give the matrices E and D for the $N = 6$ case.

Equations (48), (53), and (54) reduce equation (12) to

$$A\dot{\boldsymbol{a}} = f\left(\boldsymbol{x}, R, p, \dot{p}, BE\boldsymbol{a}, AD\boldsymbol{a}\right) \tag{55}$$

where $\boldsymbol{x} = [x_0, x_1, \ldots, x_N]^\top$. To satisfy the boundary condition (5), which corresponds to $\sum_{n=0}^{N} a_n T_{2n}(x_0) = 0$, we replace the first element of f with 0.

Given some initial condition $\boldsymbol{a}_0$, this system of ordinary differential equations, along with equations (1) and (2), can now be solved and stepped forward in time to find any later $\boldsymbol{a}$. This was done by using MATLAB's ode45 solver along with MATLAB's left division of A into f at every timestep.

To convert the collocation coeffients into a temperature distribution we use $\tau = A\boldsymbol{a}$ and then evaluate (9).

4 Results

4.1 Periodic forcing

In this section we set the ambient pressure to oscillate so as to drive the bubble. That is, we let

$$p_A(t) = p_\infty\left(1 - \epsilon \sin \omega t\right) \tag{56}$$

where P_∞ is the static pressure, ϵ is a dimensionless quantity that controls the amplitude of the pressure waves, and ω is the angular frequency.

In what follows we take the initial radius of the bubble to be $R_0 = 10\,\mu$m and the initial bubble wall velocity to be $\dot{R}_0 = 0$. We let the initial temperature inside the bubble be uniform at T_∞, which corresponds to the collocation coefficient vector $\boldsymbol{a}_0 = \boldsymbol{0}$. The other properties used were $\omega = 3.91 \cdot 10^5\,\mathrm{s}^{-1}$, $\gamma = 1.4$, $c_L = 1490\,\mathrm{m/s}$, $\mu_L = 7.98 \cdot 10^{-4}\,\mathrm{Pa\,s}$, $\rho_L = 997\,\mathrm{kg/m^2}$, $S = 7.12 \cdot 10^{-2}\,\mathrm{N/m}$, $p_\infty = 101325\,\mathrm{Pa}$, and $T_\infty = 300\,\mathrm{K}$. In figures 1, 2, and 3, the results for the $N = 6$ case are shown. In figure 4, a finer resolution of the temperature distribution was made by letting $N = 16$.

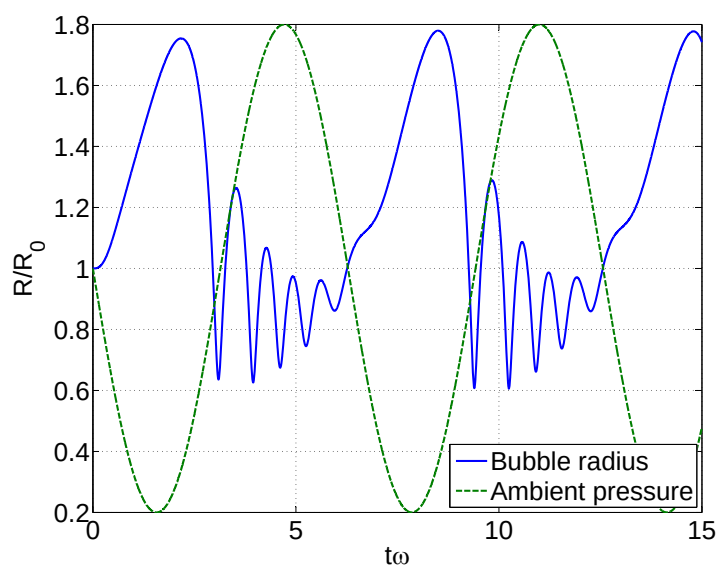

Figure 1: Bubble radius versus time for a pressure amplitude $\epsilon = 0.8$. The ambient pressure function is overlaid in dashed lines.

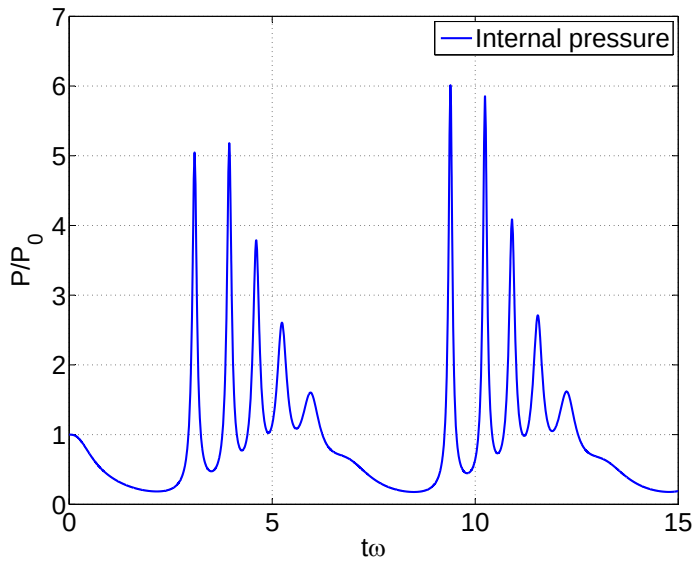

Figure 2: Internal bubble pressure versus time for the case in Figure 1.

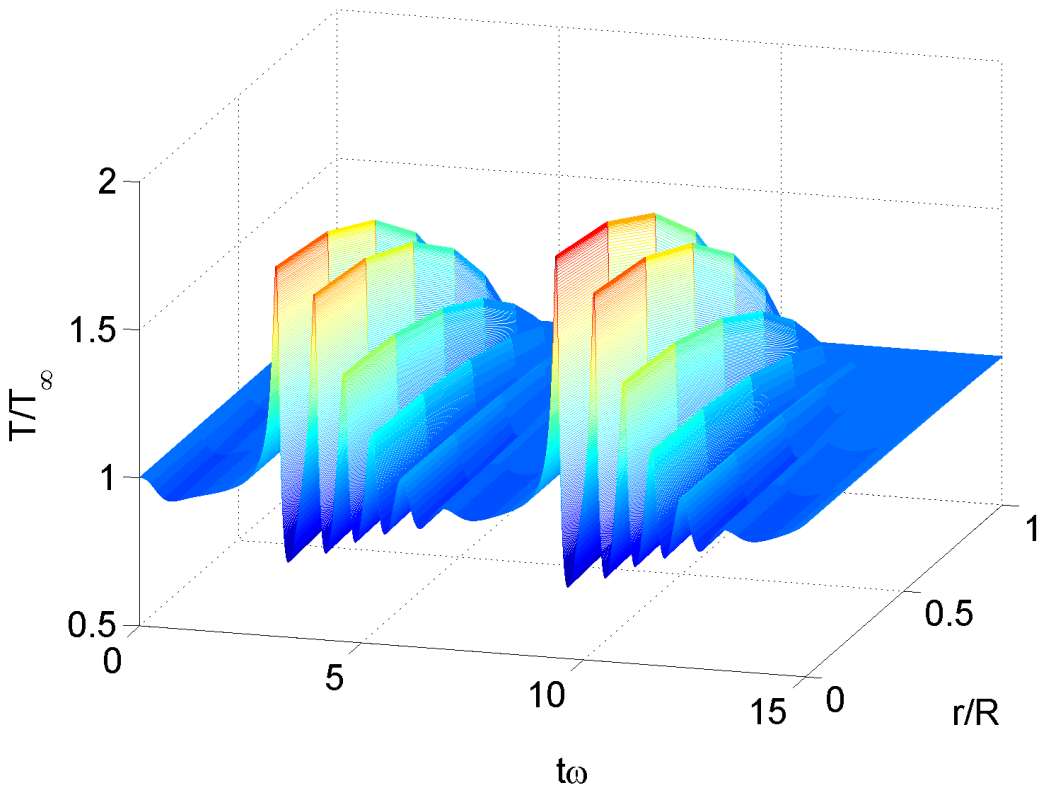

Figure 3: The temperature distribution versus time for the setup of Figures 1 and 2. The number of collocation points used was $N + 1 = 6 + 1$.

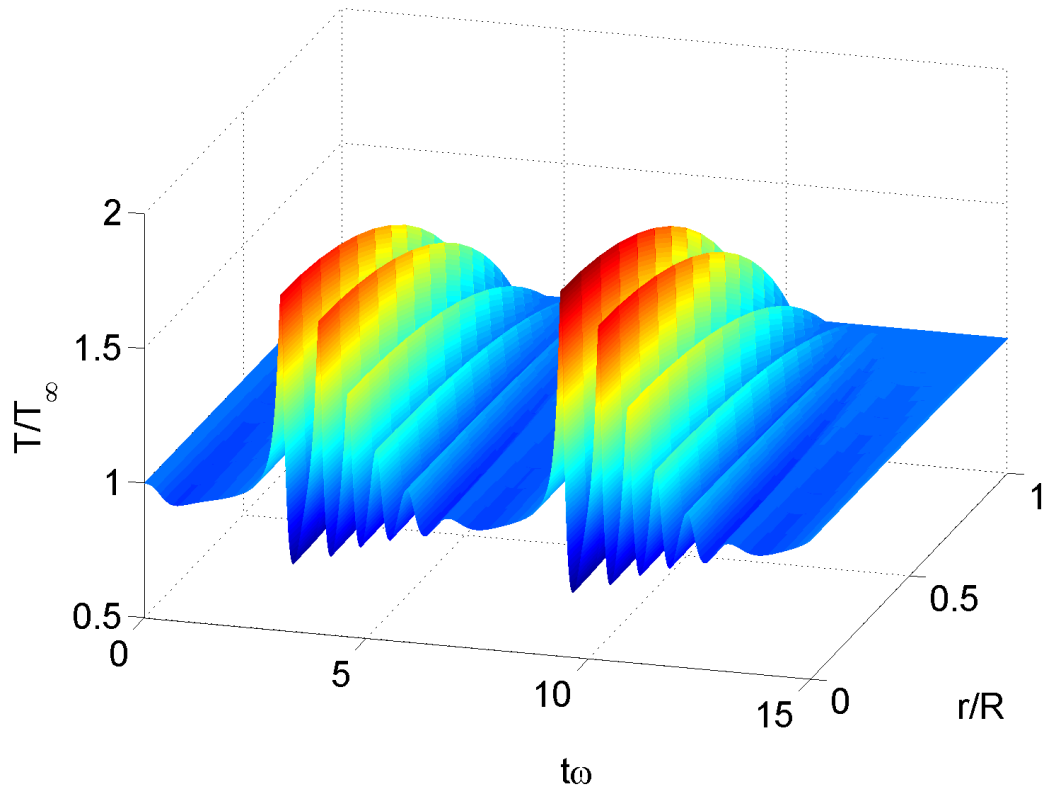

Figure 4: The temperature distribution versus time for the setup of Figures 1 and 2, but with $N = 16$.

It is worthwhile to compare these results to the polytropic approach in which the temperature in the bubble is taken to be uniform and the bubble pressure is described by

$$p = \left(p_\infty + \frac{2S}{R}\right)\left(\frac{R_0}{R}\right)^{3\gamma} \tag{57}$$

Figure 5 shows the striking difference between the two models, which has been previously observed by Prosperetti (1988). It verifies Prosperetti's result that the PDE model predicts more violent cavitation - larger maximum radii and smaller minimum radii.

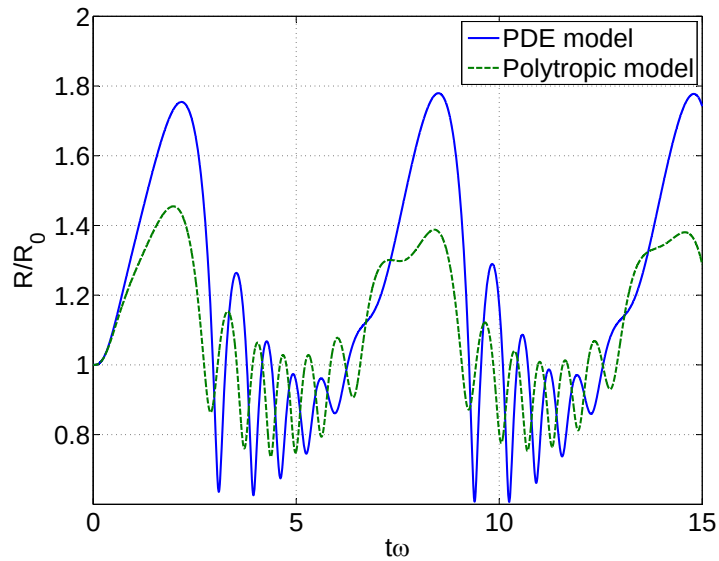

Figure 5: Radius versus time curves given by the collocation model and the polytropic model under the same conditions.

4.2 Gaussian bump

An alternative ambient pressure versus time function often used in bubble dynamics numerics is the Gaussian bump

$$p_A(t) = p_\infty \left[1 - \epsilon \exp\left(-\left(t - t_0\right)^2\right)\right] \tag{58}$$

where the time t_0 is large enough so that $p_A(0) \approx p_\infty$.

Figure 6 shows the radius versus time curve for both the collocation model and the polytropic model. Again, the collocation model predicts more violent cavitation, however, since it incorporates the effects of diffusive heat transfer, it also predicts more damping.

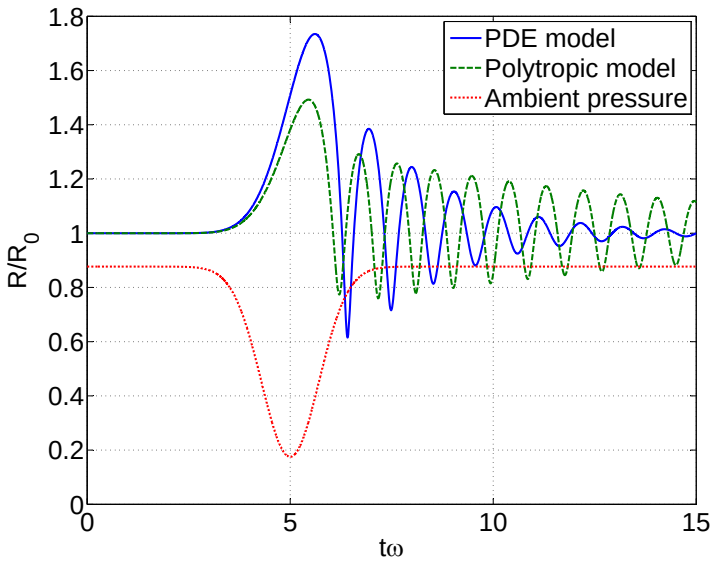

Figure 6: Radius versus time curves given by the collocation model and the polytropic model under the influence of a Gaussian pressure drop. The form of the pressure drop is overlaid.

5 Conclusions

This work serves as a successful application of the principals of collocation to bubble dynamics. The benefits of the use of the Chebyshev polynomials were formally shown, and an efficient matrix algebra implementation was derived. The computational results affirm several of the conclusions made by previous authors in the field, in particular, that models that account for thermal behavior give vastly different results than the simpler polytropic model.

5.1 Future work

A collocation method can also be used to solve for the temperature distribution in the liquid. Whereas in this study we made the cold liquid approximation, in reality the liquid temperature T_L is governed by

$$\frac{\partial T}{\partial t} + \frac{R^2 \dot{R}}{r^2} \frac{\partial T_L}{\partial r} = D_L \nabla^2 T_L \tag{59}$$

where D_L is the liquid thermal diffusivity. By using the coordinate transformation

$$\xi = \frac{l}{r/R - 1 + l} \tag{60}$$

where l is a measure of the thermal diffusion length, the domain $[R, \infty)$ is projected onto $[0, 1]$. As seen previously, the domain $[0, 1]$ lends itself easily to collocation through the Chebyshev polynomials.

Another area of future work is to apply these methods to solve bubble dynamics equations that model the effects of nonlinear viscoelasticity. Solving these equations involves integrating over the shear stress field in the surrounding viscoelastic medium. Just as recurrence relations for the Chebyshev polynomials allowed easy computation of derivatives, the same may be so for integration.

6 Appendix

For the $N = 6$ case, the matrices is equations (53) and (54) are

$$E = \begin{bmatrix} 0 & 4 & 8 & 12 & 16 & 20 & 24 \\ 0 & 0 & 8 & 12 & 16 & 20 & 24 \\ 0 & 0 & 0 & 12 & 16 & 20 & 24 \\ 0 & 0 & 0 & 0 & 16 & 20 & 24 \\ 0 & 0 & 0 & 0 & 0 & 20 & 24 \\ 0 & 0 & 0 & 0 & 0 & 0 & 24 \end{bmatrix} \tag{61}$$

$$D = \begin{bmatrix} 0 & 4 & 32 & 108 & 256 & 500 & 864 \\ 0 & 0 & 48 & 192 & 480 & 960 & 1680 \\ 0 & 0 & 0 & 120 & 384 & 840 & 1536 \\ 0 & 0 & 0 & 0 & 224 & 640 & 1296 \\ 0 & 0 & 0 & 0 & 0 & 360 & 690 \\ 0 & 0 & 0 & 0 & 0 & 0 & 528 \\ 0 & 0 & 0 & 0 & 0 & 0 & 0 \end{bmatrix} \tag{62}$$

7 References

- V. Kamath and A. Prosperetti, "Numerical integration methods in gas-bubble dynamics," J. Acoust. Soc. Am. **85**, 1538-1548 (1989).
- A. Prosperetti, L. Crum, and K. Commander, "Nonlinear bubble dynamics" J. Acoust. Soc. Am. **83**, 502 (1988).
- L. Stricker and A. Prosperetti, "Validation of an approximate model for the thermal behavior in acoustically driven bubbles," J. Acoust. Soc. Am. **130**, 3243-3251 (2011).